Sciencexpress Research Article

# The Structure and Receptor-Binding Properties of the 1918 Influenza Hemagglutinin

S.J. Gamblin,* L.F. Haire,* R.J. Russell,* D.J. Stevens, B. Xiao, Y. Ha,[‡º] N. Vasisht, D.A. Steinhauer,[#] R.S. Daniels, A. Elliot,

D.C. Wiley,[‡] J.J. Skehel[†]

MRC National Institute for Medical Research, The Ridgeway, Mill Hill, London NW7 1AA.
[‡]Department of Molecular & Cellular Biology, Howard Hughes Medical Institute, Harvard University, 7 Divinity Avenue, Cambridge, MA 02138, USA.
ºPresent address: Department of Pharmacology, Yale University School of Medicine, 333 Cedar Street, New Haven, CT 06520, USA.
[#] Present address: Department of Microbiology and Immunology, Emory University School of Medicine, 1510 Clifton Road, Atlanta, Georgia 30322, USA.

*These authors contributed equally to this work.

† To whom correspondence should be addressed: MRC National Institute for Medical Research, The Ridgeway, Mill Hill, London NW7 1AA. Email: mbrenna@nimr.mrc.ac.uk.

**The 1918 influenza pandemic resulted in about 20 million deaths. This enormous impact, coupled with renewed interest in emerging infections, makes characterisation of the virus involved a priority. Receptor binding, the initial event in virus infection, is a major determinant of virus transmissibility that for influenza viruses is mediated by the hemagglutinin membrane glycoprotein (HA). We have determined the crystal structures of the HA from the 1918 virus and of two closely related HAs in complex with receptor analogs. They explain how the 1918 HA, while retaining receptor-binding site amino acids characteristic of an avian precursor HA, is able to bind human receptors and how, as a consequence, the virus was able to spread in the human population.**

The HAs of influenza viruses mediate receptor binding and membrane fusion, the first stages of virus infection (*1*). The receptors that they recognize are sialic acids of cell-surface glycoproteins and glycolipids and the nature of the interactions involved in determining binding specificity have been described in biochemical, genetic, and structural studies (*2*–*8*). Sialic acids are usually found in either α2,3- or α2,6-linkages to galactose, the predominant penultimate sugar of N-linked carbohydrate side-chains. The binding preference of a given HA for one or other of these linkage types correlates with the species specificity for infection. Thus the HAs of all 15 antigenic subtypes found in avian influenza viruses bind preferentially to sialic acid in α2,3-linkage (*9*) and it is this form of the sialosaccharide that predominates in avian enteric tracts where these viruses replicate (*10*). Swine influenza viruses are reported to bind sialic acid in α2,6- and sometimes also in α2,3-linkage (*11*) and sialic acid in both linkages is detected in porcine trachea (*10*). Human viruses of the H1, H2, and H3 subtypes that are known to have caused pandemics in 1918, 1957, and 1968 respectively, recognize α2,6-linked sialic acid (*5*), the major form found on cells of the human respiratory tract (*12*, *13*).

Since an avian origin is proposed for the HAs of swine and human viruses (*14*), changes in binding specificity are required for cross species transfer. The mechanism that human viruses have used to achieve these changes appears to be different for different subtypes. For the HAs of the H2 and H3 human viruses a minimum of two changes in receptor-binding site amino acids, Gln-226->Leu and Gly-228->Ser, correlates with the shift from avian to human receptor binding (*15*, *16*). By contrast, HAs of human H1 viruses acquire the ability to bind to human receptors while retaining Gln-226 and Gly-228 (*11*). To understand how they do this we have determined the structures of HAs from the 1918 pandemic virus (1918-human) using HA expressed from DNA of the same sequence as that recovered from tissues infected with virus in 1918 (*17*), and from the prototype human (1934-human) and swine (1930-swine) H1 influenza viruses, A/Puerto Rico/8/34 and A/swine/Iowa/30 respectively (Fig. 1). A/Puerto Rico/8/34 was one of the first human influenza viruses isolated in the Americas (*18*) and has been widely used in laboratory investigations of influenza. A/swine/Iowa/30 was the first influenza virus isolated from mammals, in 1930 (*19*), three years before the first isolate was recovered from humans (*20*).

**Overall Structure.** The structures were solved by molecular replacement and crystallographic statistics are given in tables 1 and S1. The overall trimeric structures of the three H1 HAs are similar (Fig. 2), but they show significant differences to HAs of other subtypes with respect to the arrangements of the receptor-binding, vestigial esterase, and membrane fusion subdomains, both within the HA trimer and also within individual monomers (*21*) (table S2). As predicted from their placement in the same phylogenetic and structure-based clade, the H1 HAs are most similar to those of the H5 subtype (*21*). We have examined the structures in detail in relation to their receptor-binding and membrane fusion activities and to the antigenic variation that occurred in both periods of human H1 virus prevalence, 1918 – 1957 and 1977 – date (Fig. 2) and we will present a detailed description of this analysis elsewhere (Russell *et al.*, in preparation). We have, however, concluded that the receptor-binding properties are the most distinctive features of the 1918 virus HA and we focus on these here.

**The receptor-binding subdomain.** The receptor-binding sites are located at the membrane-distal tip of each subunit of the HA trimer (Fig. 2). Three secondary structure elements; the 190-helix (residues 190-198), the 130-loop (residues 135-138) and the 220-loop (residues 221-228) form the sides of each site with the base made up of the conserved residues Tyr-98, Trp-153, His-183 and Tyr-195 (*1*) (Fig. 2B). The conformations adopted by the 130- and 220-loops of the three H1 HAs are similar but they are significantly different from those of the equivalent loops in the HAs of other influenza subtypes (*2*, *3*) (Fig. 4 and table S2). To understand the structural basis of the receptor specificity of H1 HAs we determined the structures of the 1934-human and the 1930-swine HAs in complex with α2,3- and α2,6-linked sialopentasaccharides, as analogs of avian and human receptors respectively (*2*) (Fig. 3, S1 and S2). As observed with other HAs (*1*, *3*, *8*), the terminal sialic acids of the human and avian receptors interact with binding site residues through a series of conserved hydrogen bonds (Fig. 3, fig. S2).

**The 1934-human HA/human receptor complex.** The electron density maps reveal well-ordered features for the Sia-1, Gal-2 and GlcNAc-3 of the sialopentasaccharide in this complex (Fig. 3A and S1 and S2). Gal-2 forms five hydrogen bonds that have not been previously observed in other HA/receptor complexes. Four bonds are possible between the 2- and 3-hydroxyls of Gal-2 and the side-chains of Lys-222 and Asp-225, and a fifth between the 4-hydroxyl of Gal-2 and the main-chain amide 227 that is mediated by a water molecule.

**The 1934-human HA/avian receptor complex.** Again only the Sia-1, Gal-2 and GlcNAc-3 moieties of the sialopentasaccharide are ordered in this complex (Fig. 3B and S1 and S2). This observation is consistent with the results of hemagglutination assays showing dual binding specificity for this HA (*5*, *11*). The side-chain carbonyl of Gln-226 forms a hydrogen bond with the 4-hydroxyl of Gal-2, as observed in other HA-avian receptor complexes (*3*). In addition, there is a novel water-mediated interaction between the 4-hydroxyl of Gal-2, the main chain carbonyl of residue 225, and the side chain of Lys-222 (Fig. 3B).

**The 1930-swine HA/human receptor complex.** The sialic acid of the receptor is located similarly in the 1930-swine and 1934-human HA receptor binding sites but in the 1930 swine complex all five saccharides of the receptor analog are detected (Fig. 3C and S1 and S2). Lys-222 again forms hydrogen bonds with the 2- and 3-hydroxyls of Gal-2, although in this case Gal-2 sits higher in the binding site. Asp-190 hydrogen bonds to the amino nitrogen of GlcNAc-3, Ser-193 hydrogen bonds to the 2-hydroxyl of Gal-4 and there is a water-mediated interaction between Thr-189 and GlcNAc-5. The last three interactions have not been observed before in HA receptor complexes. In addition, the sialopentasaccharide exits the binding site in an orientation not previously seen, crossing the 190-helix near its N-terminus, approximately parallel to the three-fold symmetry axis of the HA trimer (Fig. 3C).

**The 1930-swine HA/avian receptor complex.** The electron density for the avian receptor analog bound to the 1930-swine HA is weak and mainly represents the sialic acid moiety (Fig. 3D and S1 and S2). A similar situation was observed for an H5 avian HA in complex with a human receptor analog where only a subset of the atoms for the sialic acid could be located (*3*). These observations probably reflect the low affinity of the HAs for their respective ligands, consistent with the preference of the 1930 swine virus for human receptor in hemagglutination assays as detailed in reference 11.

To ascertain the essential differences in the binding sites that allow the "avian" binding site structure of H1 HAs to recognise both human and avian receptors, we have compared their structures with those of H3 avian (A/duck/Ukraine/63) and human (X-31) HAs, determined before, that prefer either avian (*22*) or human receptors (*2*).

**Human receptor complexes.** Complexes of human receptor analog bound to 1934-human HA (green) and 1930-swine HA (blue) and to human H3 HA (red) are superposed in Figure 4A. Perhaps the most important feature arising from this comparison is the difference in structure adopted by the 130- and 220-loops of the receptor-binding site between the H1 and H3 HAs. One consequence of the change in the 130-loop structure is that the sialic acid of the receptor is tilted about 10º into the receptor binding sites of the H1 HAs. This effect, together with different orientations about the glycosidic bond, contributes to Gal-2 being located almost 2Å

lower in the H1 HAs than in the human H3 HAs. Gal-2 is able to adopt this position because structural differences in the 220-loop locate Gln-226 lower in the binding site than the equivalent Leu-226 of human H3 HA. Consequently, in the H1 HAs Gal-2 is located closer to the 220-loop and is able to form hydrogen bonds with Lys-222. In the case of the 1934-human HA, Gal-2 also interacts with Asp-225. Thus a combination of factors relating to the structure of the 130- and 220-loops enable the H1 HAs to make favourable hydrogen bond interactions with Gal-2 of the human receptor. Gln-226 plays an essentially passive role in this process in marked contrast to the role played by Leu-226 in the binding of human H3 HA to human receptor. In that case, Gal-2 makes hydrophobic contacts with Leu-226 and the higher position and the nature of this side chain are important for human receptor binding (*2*, *22*).

**Avian receptor complexes.** Complexes of avian receptor analogues with 1934-human HA (green), 1930-swine HA (blue) and an avian H3 HA (red) (*22*) are overlaid in Figure 4B. Again the differences in the structure of the 130-loop between the H1 and H3 HAs result in the sialic acid of the avian receptor being located lower in the receptor binding site of the H1 HAs. Comparison of the 1934-human and avian H3 complexes also reveals that Gal-2 of the avian receptor is located about 1Å lower in the binding site of the H1 complex, as is Gln-226. In both complexes, the 4-hydroxyl of Gal-2 hydrogen bonds with the side-chain carbonyl of Gln-226 (Fig. 3B) and the coordinated differences in position of the bound receptor and Gln-226 enable this interaction to be conserved. It seems therefore that 1934-human HA is able to bind avian receptor in a manner reminiscent of avian HAs (*3*), with Gln-226 playing a key role.

Given that the overall structure of 1930-swine and 1934-human HA receptor binding sites are very similar (Fig. 2B), and that both contain a glutamine residue at position 226, why does the 1930-swine HA bind less effectively to avian receptors than 1934-human HA? The reason seems to be that the position adopted by Gln-226 in 1934-human HA is about 1Å higher in its complex with the avian receptor than it is in either the human receptor complex or uncomplexed (Fig. 5). By contrast, the position of Gln-226 in 1930-swine HA is approximately the same uncomplexed and in the human and avian receptor complexes. The apparent inability of Gln-226 to adopt a higher position in the receptor-binding site seems to explain the failure of 1930-swine HA to interact as effectively with the avian receptor. This explanation is supported by the structural observation that in the 1934-human HA complex with avian receptor, Glu-190 interacts through two water molecules with Gln-226 (Fig. 5). This network of hydrogen bonds may be necessary to position Gln-226 in the binding site for its interaction with Gal-2. Glu-190 is conserved in avian H1 HAs, all of which specifically bind α2,3-linked receptors. By contrast, residue 190 of 1930-swine HA is an aspartic acid which does not interact with either the 9-hydroxyl of Sia-1 or with Gln-226 and is thus unable to facilitate binding to avian receptor.

Many of the viruses from the first H1 influenza pandemic period, 1918-1957, recognized to some extent, both avian and human receptors while those from the second period, 1977-date, appear to be more human receptor-specific (*11*). Loss of the ability to bind avian receptors, which may be an advantage in the face of infectivity-blocking α2,3-linked soluble sialosides in human lungs (*13*), was proposed to correlate with the amino acid substitution Ala-138->Ser (*11*). Our structural data also support this interpretation since an interaction between Ser-138 and Gln-226 is feasible and would favour the lower positioning in the receptor binding site of Gln-226 and the consequent negative effect on avian receptor binding.

**The receptor binding specificity of the 1918-human HA.** Although we have been unable to obtain receptor analog complexes with the 1918 HA, we can deduce its likely specificity based on our observations of receptor binding to 1930-swine and 1934-human HAs. Table 2 compares potentially important contact residues in the receptor binding sites of 1934-human, 1930-swine, 1918-human, and a representative avian H1 HA (*9*). From these data, and the close similarity of the structures of the human and swine HA binding sites (Fig. 2), two of the five HAs reported from 1918 viruses (*17*, *23*) have receptor-binding sites, and presumably binding specificities, indistinguishable from those of 1930-swine HA. The other three 1918 HAs which differ only at residue 225 (Table 2) most likely also prefer binding to human rather than avian receptors. If interactions with Lys-222 and Asp-225 are formed with human receptors, as in the 1934-human HA complex, then the overall orientation of the oligosaccharide in the 1918 HA binding sites may also be similar. In this case, Asp-190 would not contact the amino-group of GlcNAc-3 and the entire complex would closely resemble that formed by the 1934-human HA rather than by the 1930-swine HA. However, the fact that Asp-190 is often conserved in human H1 HAs (*24*), as is Ser-193, suggests that in the 1918 HA and in H1 HAs generally, these residues interact with GlcNAc-3 and Gal-4 in similar ways to those seen in the 1930-swine HA-human receptor complex. This conclusion is also consistent with the ability of human H1 HAs to discriminate between the receptor analogs 6'sialyllactosamine and 6'sialyllactose that is reported to be dependent on Asp-190 (*25*, *26*).

Irrespective of the single amino acid difference, Asp- or Gly- at residue 225 (Table 2) between the sequences of 1918-human HAs, by recognizing human receptors they would all contribute the first requirement of an epidemic virus – the ability to spread in the human population. The importance of

this requirement was emphasized in the 1997 outbreak of H5 "chicken" influenza in Hong Kong when the virus was extremely virulent, but did not acquire the ability to bind α2,6-linked sialosides (*27*) and was therefore unable to spread. With the ability to ensure the efficiency of the initial stages of virus infection, coupled with novel antigenicity, the human-1918 HA may have been the prime determinant of extensive mortality in the 1918 pandemic.

**References and Notes**


1. J. J. Skehel, D. C. Wiley, *Annu Rev Biochem* **69**, 531 (2000).
2. M. B. Eisen, S. Sabesan, J. J. Skehel, D. C. Wiley, *Virology* **232**, 19 (1997).
3. Y. Ha, D. J. Stevens, J. J. Skehel, D. C. Wiley, *Proc. Natl. Acad. Sci. USA* **98**, 11181 (2001).
4. M. Matrosovich *et al.*, *J Virol* **74**, 8502 (2000).
5. G. N. Rogers, J. C. Paulson, *Virology* **127**, 361 (1983).
6. G. N. Rogers *et al.*, *Nature* **304**, 76 (1983).
7. N. K. Sauter *et al.*, *Biochemistry* **28**, 8388 (1989).
8. W. Weis *et al.*, *Nature* **333**, 426 (1988).
9. E. Nobusawa *et al.*, *Virology* **182**, 475 (1991).
10. T. Ito *et al.*, *J Virol* **72**, 7367 (1998).
11. G. N. Rogers, B. L. D'Souza, *Virology* **173**, 317 (1989).
12. L. G. Baum, J. C. Paulson, *Acta Histochem Suppl* **40**, 35 (1990).
13. J. N. Couceiro, J. C. Paulson, L. G. Baum, *Virus Res* **29**, 155 (1993).
14. R. G. Webster, *Proc Natl Acad Sci U S A* **96**, 1164 (1999).
15. C. W. Naeve, V. S. Hinshaw, R. G. Webster, *J Virol* **51**, 567 (1984).
16. R. J. Connor, Y. Kawaoka, R. G. Webster, J. C. Paulson, *Virology* **205**, 17 (1994).
17. A. H. Reid, T. G. Fanning, J. V. Hultin, J. K. Taubenberger, *Proc Natl Acad Sci U S A* **96**, 1651 (1999).
18. T. Francis, *Science* **80**, 457 (1936).
19. R. E. Shope, *J. Exp. Med.* **54**, 373 (1931).
20. W. Smith, Andrewes, C.H. and Laidlaw, P.O., *Lancet* **1**, 66 (1933).
21. Y. Ha, Stevens, D.J., Skehel, J.J. and Wiley, D.C., *Embo J* **21**, 865 (2002).
22. Y. Ha, D. J. Stevens, J. J. Skehel, D. C. Wiley, *Virology* **309**, 209 (2003).
23. A. H. Reid *et al., Emerg. Inf. Dis.* **9**, 1249 (2003).
24. F. L. Raymond, A. J. Caton, N. J. Cox, A. P. Kendal, G. G. Brownlee, *Nucleic Acids Res* **11**, 7191 (1983).
25. M. N. Matrosovich *et al.*, *Virology* **196**, 111 (Sep, 1993).
26. A. S. Gambaryan *et al.*, *Virology* **232**, 345 (Jun 9, 1997).
27. M. Matrosovich, Zhou, N., Kawaoka, Y. and Webster, R., *J. Virol.* **73**, 1146 (1999).
28. M. Bennett, Gregory, V., Y.-P. Lin, A.J. Hay., unpublished data.


29. We thank S. Smerdon and P. Walker for assistance and discussion. Diffraction data were collected at SRS Daresbury and ESRF Grenoble. We thank J. Nicholson (SRS) and S. McSweeney (ESRF) for rapid access to, and assistance with, beamtime as well as other beamline staff. This research was supported by the MRC (UK), NIH Grant AI-13654 and by a supplement to this grant for Expanded International Research on Emerging and Re-Emerging Diseases, by an International Partnership Research Award in Veterinary Epidemiology of the Wellcome Trust and by the Howard Hughes Medical Institute. The coordinates for the 1918-human, 1934-human, 1934-human/human, 1934 human/avian, 1930-swine, 1930-swine/human and 1930-swine/avian HAs have been deposited in the Protein Data Bank (accession codes 1RUZ, 1RU7, 1RVZ, 1RVX, 1RUY, 1RVT, 1RV0.


**Supporting Online Material**

www.sciencemag.org/cgi/content/full/1093155/DCI
Materials and Methods
Figures S1 and S2
Tables S1 to S3
References and Notes


30 October 2003; accepted 7 January 2004
Published online 5 February 2004; 10.1126/science.1093155
Include this information when citing this paper.


**Fig. 1.** Sequence alignment of 1918-human, 1930-swine and 1934-human HAs. The sub-domain structure of HA in the two polypeptides, HA1 and HA2, that form each monomer, is indicated by the coloured bars above the sequences. Carbohydrate attachment sites are shaded grey. Residue numbering is based on H3 HA sequence (*1*).

**Fig. 2.** Structures of 1918-human, 1934-human and 1930-swine HAs. (**A**) Ribbons diagram of the trimer of 1918-human HA. Monomers 2 and 3 are in silver and gold respectively, and the featured monomer is colored according to its individual subdomains as in Fig. 1: receptor-binding (RB) in blue, vestigial esterase (E) in yellow, fusion subdomains (F´ and F) in magenta and red respectively (*21*). Changes in the relative orientations of individual subdomains of H1 HA relative to H3 HA can usefully be described (*21*) after superposing the two structures using just the F domain. The RB, E and F´ subdomains of H1 are related to the equivalent subdomains in H3 by a clockwise rotation of 23° about the trimer three-fold axis. Glycosylation sites are indicated by spheres; in green are those observed in the 1918-human HA (21, 33, 94 and 289 in the F´ and E subdomains and 154 in the F subdomain) and in red are the sites (63,

81,129 or 131, 158, 163 and 271 in the F´, E and RB subdomains) that have accumulated on the membrane distal surface between 1918 and 2002 (*17, 24, 28*) that probably influence antigeniicity. (**B**) An expanded view of the superposed polypeptide backbone of the receptor binding site of all three H1 HAs. The position of the three secondary structure units making up the site, the 190-helix and the 130- and 220-loops are indicated. Also shown are the side chains of some residues important for receptor binding. Certain Cα positions are indicated by black spheres for residues discussed in the text. Overall, the three H1 structures are very similar with r.m.s.d on all Cα of 0.82 Å and 0.56 Å for 1918-human versus 1934-human and 1930-swine respectively. (**C**) An expanded view of a region of the F subdomain indicating differences between H1 and H5 subtype HAs in the position of the loop connecting helix A to helix B. Since H1 and H5 are in the same phylogenetic clade, these differences imply that the position of the interhelical loop relative to helix B is not a clade-specific feature as suggested previously (*21*). Interactions between the C-terminal region of the loop and the RB and E subdomains (110-helix) influence the dispositions of the subdomains relative to the central coiled-coil formed in the trimer by the B-helices.

**Fig. 3.** Interactions of 1934-human HA (upper panels) and 1930-swine HA (lower panels) with human receptor and with avian receptor analogs. The view of the receptor binding site is approximately the same as in Figure 2B. The three secondary structure components of the binding site are labelled in this backbone representation together with some of the most relevant side chains. The broken lines indicate potential hydrogen bond interactions between the protein and the receptors, residues making interactions via main chain carbonyl groups are shown as red spheres while those interacting via main chain nitrogens are shown as blue spheres. In all four panels the sialosaccharides are colored yellow for carbon atoms, blue for nitrogen and red for oxygen. Water molecules are indicated by green spheres. (**A**) 1934-human HA in complex with human receptor and (**B**) 1934-human HA in complex with avian receptor, in both cases the HA is colored in green for backbone and carbon atoms. (**C**) 1930-swine HA in complex with human receptor and (**D**) 1930-swine HA in complex with avian receptor, in this case the backbone and carbon atoms of the HA are colored in blue. The small black arrows in (A), (B) and (C) are to indicate that for the two human receptor complexes the Sia-1-Gal-2 linkage adopts a *cis* conformation about the glycosidic bond while for the avian complex it adopts a *trans* conformation. The large black arrow in (**C**) indicates the direction of an axis parallel to the trimer three-fold axis.

**Fig. 4**. Differences in the orientations of bound receptors in the receptor-binding sites of three different HAs. The receptor binding sites of 1934-human HA (green), 1930-swine HA (blue) and human H3 HA (red) are overlayed. The view matrix is approximately the same as in Figure 3. The sialopentasaccharides are colored according to the HAs to which they are bound. The side-chains of Gln-226 (H1 HAs) and Leu-226 (H3 HA) are shown. (**A**) Human receptor complexes. (**B**) Avian receptor complexes.

**Fig. 5.** Superposition of the binding site of 1934-human HA in its uncomplexed state and complexed with avian receptor analog. The HA is shown in green in both cases and the avian receptor is colored as in Figure 3. Two water molecules, shown as green spheres, link Glu-190 to Gln-226 in the avian receptor complex. This hydrogen-bonded network is not formed in the uncomplexed structure or in the human receptor complex not shown.

**Table 1.** Crystallographic statistics. More extensive crystallographic data are given in Table S1.

| H1 HA Type | Resolution (Å) | $R_{work}$ (%) | $R_{free}$ (%) | Rmsd bonds |
|---|---|---|---|---|
| Human 1918 | 2.9 | 24.8 | 28.9 | 0.007 |
| Swine 1930 uncomplexed | 2.7 | 24.8 | 26.5 | 0.006 |
| + avian receptor | 2.5 | 21.4 | 25.4 | 0.006 |
| + human receptor | 2.5 | 21.7 | 25.4 | 0.007 |
| Human 1934 uncomplexed | 2.3 | 23.5 | 26.6 | 0.006 |
| + avian receptor | 2.2 | 22.7 | 26.0 | 0.006 |
| + human receptor | 2.25 | 22.5 | 25.7 | 0.006 |

**Table 2.** Residue types at four positions in the receptor binding sites of 1918-human, 1930-swine, 1934-human and a representative avian H1 HA.

| Residue / HA | 1918-human | 1930-swine | 1934-human | Avian |
|---|---|---|---|---|
| **190** | Asp | Asp | Glu | Glu |
| **193** | Ser | Ser | Asn | Ser |
| **222** | Lys | Lys | Lys | Lys |
| **225** | Asp (3) /Gly (2) | Gly | Asp | Gly |

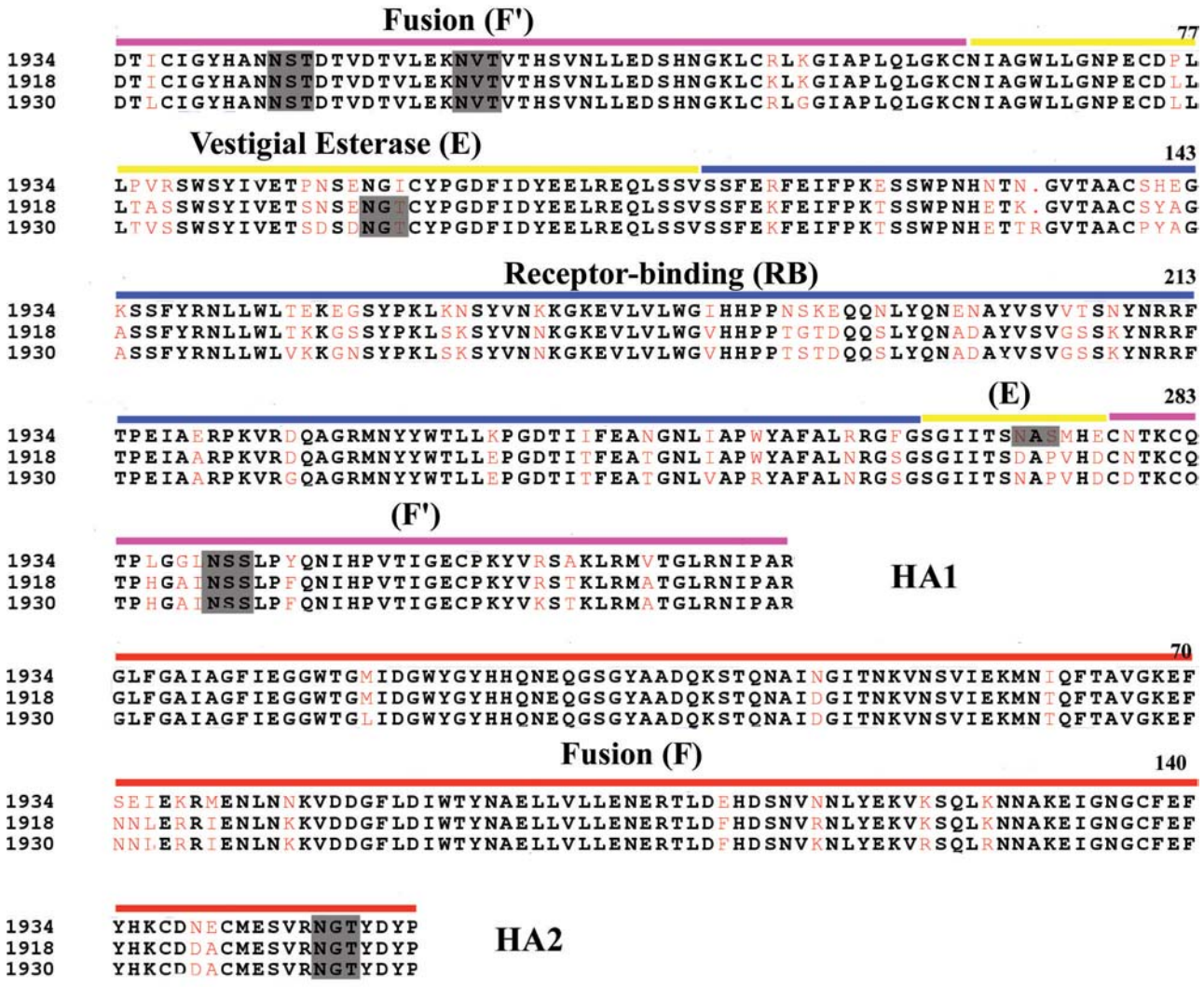
Fusion (F')
77
1934 DTICIGYHANNSTDTVDTVLEKNVTVTHSVNLLEDSHNGKLCRLKGIAPLQLGKCNIAGWLLGNPECDPL
1918 DTICIGYHANNSTDTVDTVLEKNVTVTHSVNLLEDSHNGKLCKLKGIAPLQLGKCNIAGWLLGNPECDLL
1930 DTLCIGYHANNSTDTVDTVLEKNVTVTHSVNLLEDSHNGKLCRLGGIAPLQLGKCNIAGWLLGNPECDLL
Vestigial Esterase (E)
143
1934 LPVRSWSYIVETPNSENGICYPGDFIDYEELREQLSSVSSFERFEIFPKESSWPNHNTN.GVTAACSHEG
1918 LTASSWSYIVETSNSENGTCYPGDFIDYEELREQLSSVSSFEKFEIFPKTSSWPNHETK.GVTAACSYAG
1930 LTVSSWSYIVETSDSDNGTCYPGDFIDYEELREQLSSVSSFEKFEIFPKTSSWPNHETTRGVTAACPYAG
Receptor-binding (RB)
213
1934 KSSFYRNLLWLTEKEGSYPKLKNSYVNKKGKEVLVLWGIHHPPNSKEQQNLYQNENAYVSVVTSNYNRRF
1918 ASSFYRNLLWLTKKGSSYPKLSKSYVNNKGKEVLVLWGVHHPPTGTDQQSLYQNADAYVSVGSSKYNRRF
1930 ASSFYRNLLWLVKKGNSYPKLSKSYVNNKGKEVLVLWGVHHPPTSTDQQSLYQNADAYVSVGSSKYNRRF
(E)
283
1934 TPEIAERPKVRDQAGRMNYYWTLLKPGDTIIFEANGNLIAPWYAFALRRGFGSGIITSNASMHECNTKCQ
1918 TPEIAARPKVRDQAGRMNYYWTLLEPGDTITFEATGNLIAPWYAFALNRGSGSGIITSDAPVHDCNTKCQ
1930 TPEIAARPKVRGQAGRMNYYWTLLEPGDTITFEATGNLVAPRYAFALNRGSGSGIITSNAPVHDCDTKCQ
(F')
1934 TPLGGINSSLPYQNIHPVTIGECPKYVRSAKLRMVTGLRNIPAR
1918 TPHGAINSSLPFQNIHPVTIGECPKYVRSTKLRMATGLRNIPAR
1930 TPHGAINSSLPFQNIHPVTIGECPKYVKSTKLRMATGLRNIPAR
HA1
70
1934 GLFGAIAGFIEGGWTGMIDGWYGYHHQNEQGSGYAADQKSTQNAINGITNKVNSVIEKMNIQFTAVGKEF
1918 GLFGAIAGFIEGGWTGMIDGWYGYHHQNEQGSGYAADQKSTQNAIDGITNKVNSVIEKMNTQFTAVGKEF
1930 GLFGAIAGFIEGGWTGLIDGWYGYHHQNEQGSGYAADQKSTQNAIDGITNKVNSVIEKMNTQFTAVGKEF
Fusion (F)
140
1934 SEIEKRMENLNNKVDDGFLDIWTYNAELLVLLENERTLDEHDSNVNNLYEKVKSQLKNNAKEIGNGCFEF
1918 NNLERRIENLNKKVDDGFLDIWTYNAELLVLLENERTLDFHDSNVRNLYEKVKSQLKNNAKEIGNGCFEF
1930 NNIERRIENLNKKVDDGFLDIWTYNAELLVLLENERTLDFHDSNVKNLYEKVRSQLRNNAKEIGNGCFEF
1934 YHKCDNECMESVRNGTYDYP
1918 YHKCDDACMESVRNGTYDYP
1930 YHKCDDACMESVRNGTYDYP
HA2

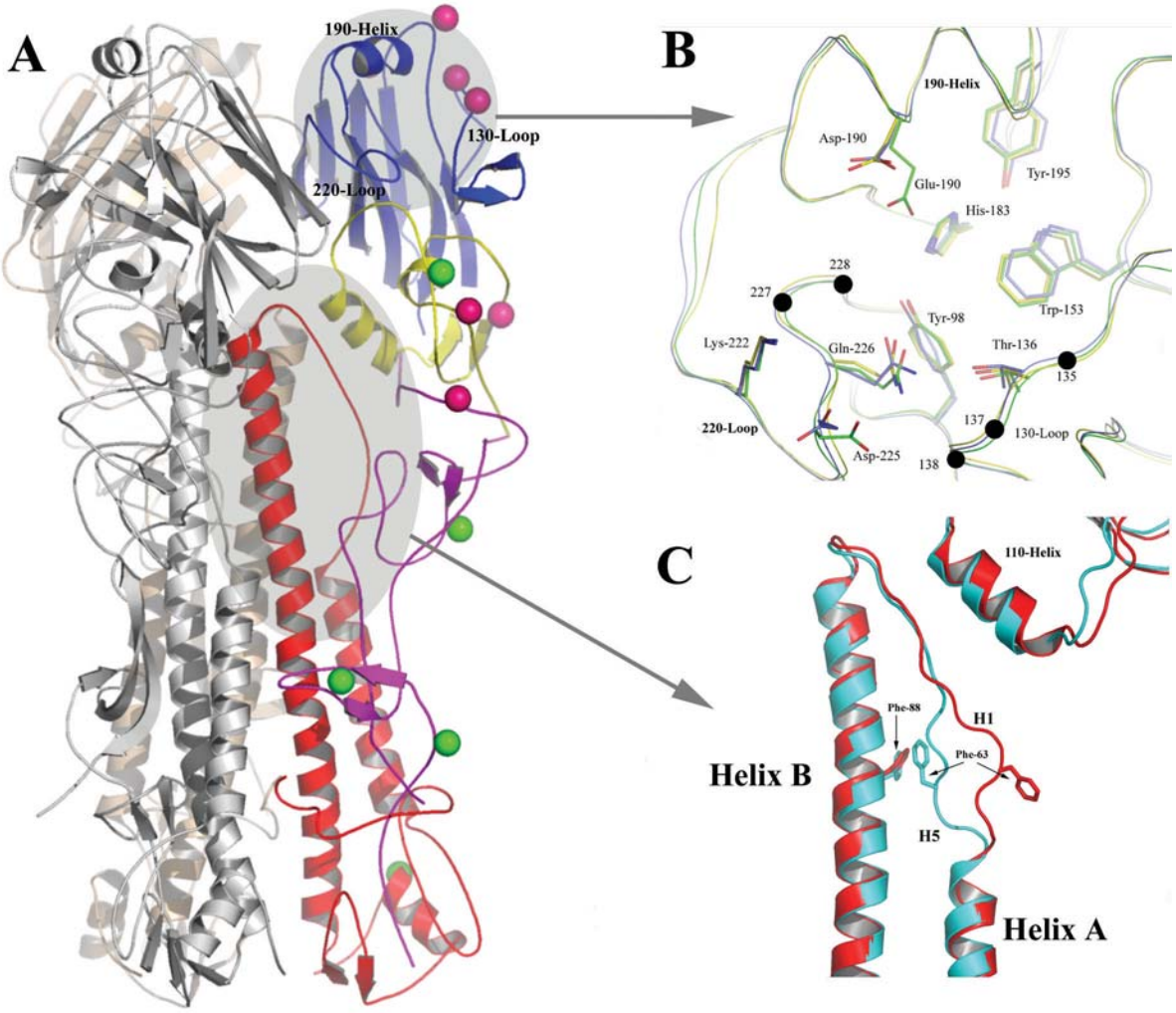
A
190-Helix
130-Loop
220-Loop
B
190-Helix
Asp-190
Glu-190
Tyr-195
His-183
228
227
Tyr-98
Trp-153
Lys-222
Gln-226
Thr-136
135
220-Loop
137
130-Loop
Asp-225
138
C
110-Helix
Phe-88
H1
Phe-63
Helix B
H5
Helix A

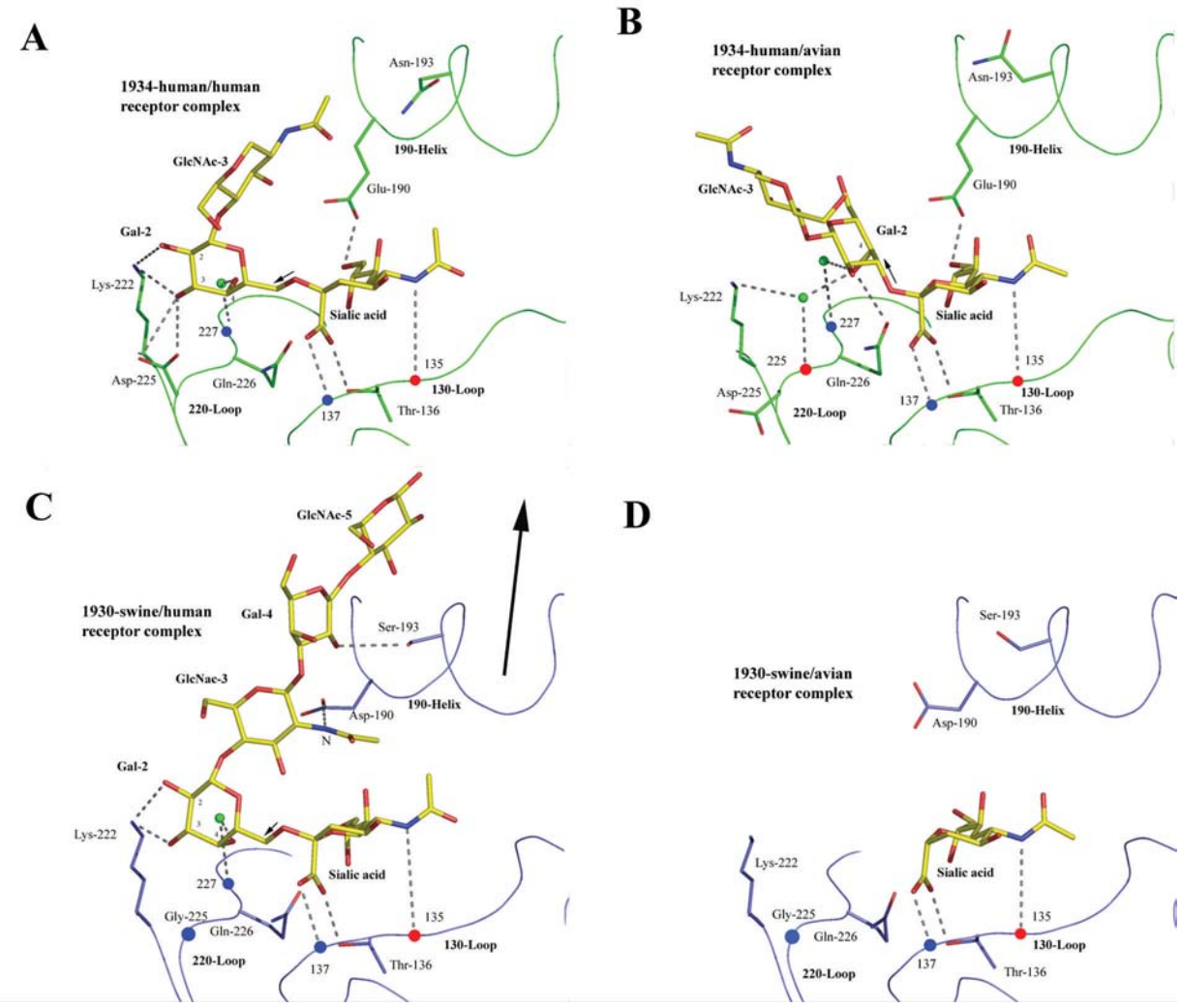
A
1934-human/human
receptor complex
Asn-193
190-Helix
GlcNAc-3
Glu-190
Gal-2
Lys-222
Sialic acid
227
Asp-225
Gln-226
220-Loop
135
130-Loop
137
Thr-136
B
1934-human/avian
receptor complex
Asn-193
190-Helix
GlcNAc-3
Glu-190
Gal-2
Lys-222
Sialic acid
227
225
Asp-225
Gln-226
220-Loop
135
130-Loop
137
Thr-136
C
1930-swine/human
receptor complex
GlcNAc-5
Gal-4
Ser-193
GlcNac-3
190-Helix
Asp-190
N
Gal-2
Lys-222
Sialic acid
227
Gly-225
Gln-226
220-Loop
135
130-Loop
137
Thr-136
D
1930-swine/avian
receptor complex
Ser-193
190-Helix
Asp-190
Lys-222
Sialic acid
Gly-225
Gln-226
220-Loop
135
130-Loop
137
Thr-136

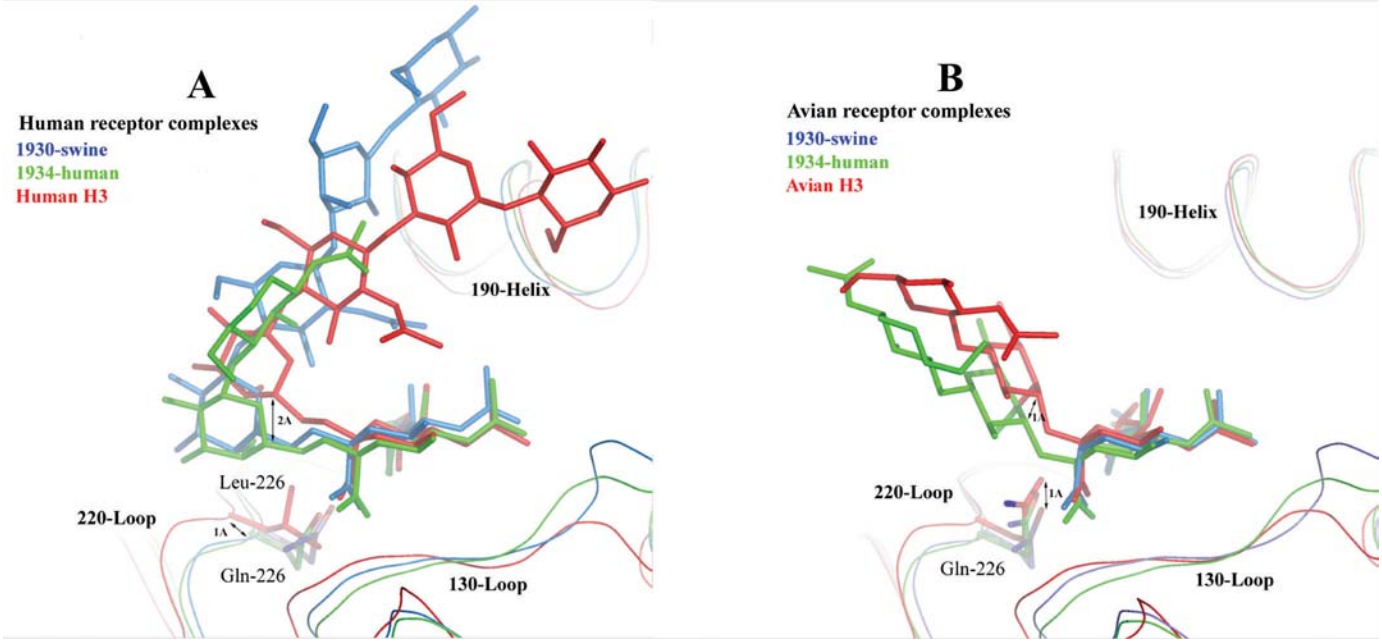
A
Human receptor complexes
1930-swine
1934-human
Human H3
190-Helix
2A
Leu-226
220-Loop
1A
Gln-226
130-Loop
B
Avian receptor complexes
1930-swine
1934-human
Avian H3
190-Helix
1A
220-Loop
1A
Gln-226
130-Loop

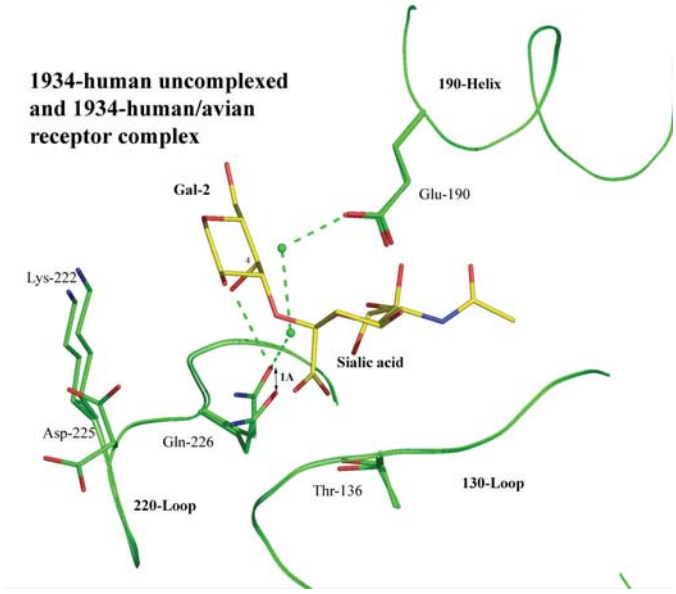
1934-human uncomplexed
and 1934-human/avian
receptor complex
190-Helix
Gal-2
Glu-190
Lys-222
Sialic acid
1A
Asp-225
Gln-226
220-Loop
Thr-136
130-Loop